

Revised assessment of cancer risk to dichloromethane II. Application of probabilistic methods to cancer risk determinations

Raymond M. David^{a,*}, Harvey J. Clewell^b, P. Robinan Gentry^c, Tammie R. Covington^c,
David A. Morgott^a, Dale J. Marino^a

^a Health and Environment Laboratories, Eastman Kodak Company, Rochester, NY 14652, USA

^b CIIT Centers for Health Research, Research Triangle Park, NC 27709, USA

^c ENVIRON Health Sciences Institute, Ruston, LA 71570, USA

Received 21 September 2005

Available online 24 January 2006

Abstract

An updated PBPK model of methylene chloride (DCM, dichloromethane) carcinogenicity in mice was recently published using Bayesian statistical methods (Marino et al., 2006). In this work, this model was applied to humans, as recommended by Sweeney et al. (2004). Physiological parameters for input into the MCMC analysis were selected from multiple sources reflecting, in each case, the source that was considered to represent the most current scientific evidence for each parameter. Metabolic data for individual subjects from five human studies were combined into a single data set and population values derived using MCSim. These population values were used for calibration of the human model. The PBPK model using the calibrated metabolic parameters was used to perform a cancer risk assessment for DCM, using the same tumor incidence and exposure concentration data relied upon in the current EPA (1991) IRIS entry. Unit risks, i.e., the risk of cancer from exposure to $1 \mu\text{g}/\text{m}^3$ over a lifetime, for DCM were estimated using the calibrated human model. The results indicate skewed distributions for liver and lung tumor risks, alone or in combination, with a mean unit risk (per $\mu\text{g}/\text{m}^3$) of 1.05×10^{-9} , considering both liver and lung tumors. Adding the distribution of genetic polymorphisms for metabolism to the ultimate carcinogen, the unit risks range from 0 (which is expected given that approximately 20% of the US population is estimated to be nonconjugators) up to a unit risk of 2.70×10^{-9} at the 95th percentile. The median, or 50th percentile, is 9.33×10^{-10} , which is approximately a factor of 500 lower than the current EPA unit risk of 4.7×10^{-7} using a previous PBPK model. These values represent the best estimates to date for DCM cancer risk because all available human data sets were used, and a probabilistic methodology was followed.

© 2006 Elsevier Inc. All rights reserved.

Keywords: Methylene chloride; Dichloromethane; Risk assessment; PBPK modeling; Bayesian analysis; Monte Carlo analysis; GST polymorphism

1. Introduction

Dichloromethane (DCM, methylene chloride) is the industrial solvent of choice for cellulose acetate production, with uses in consumer products such as paint strippers and in the decaffeinating process of coffee. In response to questions about the long-term effects of exposure to DCM, several chronic toxicity/oncogenicity studies were conducted in the late 1970s. Lung tumors were observed in mice exposed

to DCM by inhalation, and liver tumors were observed in mice exposed to DCM by inhalation or per os.

The roles of cytochrome P450 (CYP) and glutathione *S*-transferase (GST) in the metabolism of DCM were recognized as key to the development of tumors in experimental animals (reviewed in Slikker et al., 2004a,b). According to this MOA, carcinogenicity in the liver and lungs of mice is dependent upon a dose-dependent transition in metabolism from a cytochrome P450 enzyme pathway (CYP 2E1) to a glutathione *S*-transferase (GST-T1) pathway. The CYP2E1 oxidation enzymes have a high affinity for DCM; thus, this pathway predominates at low concentrations

* Corresponding author. Fax: +1 585 722 7561.

E-mail address: raymond.david@kodak.com (R.M. David).

resulting in the formation of carbon monoxide (among other metabolites) that binds to hemoglobin to form carboxyhemoglobin. This pathway is saturable as the exposure or dose is increased, shifting the metabolism of DCM to the GST pathway that has a lower affinity but higher capacity. It is at concentrations above which this shift occurs that an increase in tumors is observed in laboratory animals. Because of the dose-dependent change in metabolism (and number of tumors), the risk of carcinogenesis from exposure to DCM is non-linear (Slikker et al., 2004a).

Using this hypothesis, a PBPK model was developed for DCM by Andersen et al. (1987) to examine the importance of these metabolic pathways for tumor formation in laboratory animals and the potential implication in humans. The US Environmental Protection Agency (EPA) first estimated the risk of cancer from lifetime exposure to an airborne concentration of $1 \mu\text{g}/\text{m}^3$ DCM using a linear-multistage approach from the results of the National Toxicology Program (NTP) chronic study. Assuming that no thresholds for carcinogenesis exist, that DCM is not a genotoxic carcinogen, and that humans are more susceptible to cancer than are rodents (EPA, Guidelines for Carcinogen Risk Assessment 1986), the risk of cancer from 70 years of breathing $1 \mu\text{g}/\text{m}^3$ DCM (assuming a daily air exchange of 20m^3) was calculated to be 4.1×10^{-4} (EPA, 1985). However, following the formulation of the PBPK model of Andersen et al. (1987), the EPA adopted the use of PBPK modeling for DCM in 1991 as a reasonable means for evaluating risk by predicting target organ doses in the species of interest, and recalculated the unit risk value to be 4.7×10^{-7} (EPA, 1991). Since then, several quantitative assessments of DCM cancer risk, using the basic Andersen et al. model, have incorporated advances in scientific understanding of metabolism and statistical approaches to address variability in humans. For example, information on human GST-T1 polymorphisms was incorporated in PBPK modeling using probabilistic (Bayesian) methodology (El-Masri et al., 1999; Jonsson and Johanson, 2001). These advances have provided a means of incorporating population distributions that better reflect the likely real-world situation (Portier and Kaplan, 1989). This model for animals has recently been updated using new data for CYP-associated metabolism and using Bayesian statistics (Marino et al., 2006).

Recent models (Casanova et al., 1996; El-Masri et al., 1999; Jonsson and Johanson, 2001) have utilized DNA-protein cross-links (DPX) as dosimeters, rather than the more traditional dosimeter of mg DCM metabolized by the GST pathway/L tissue/day, and Bayesian models were calibrated on a single human exposure data set (El-Masri et al., 1999; Jonsson and Johanson, 2001). While both dose metrics are related to GST metabolism of DCM, DPX has only been demonstrated in mouse liver, not in mouse lung (the other target organ) and not in human liver (Casanova et al., 1996, 1997). Thus, extrapolation to the lung and humans has to be performed relative to metabolism by GST pathways in those tissues without the actual confirmation of a

measurable result. Of course, the argument that DPX is at least measurable in one tissue, compared with the proposed reactive chloromethylglutathione metabolite proposed in the Andersen et al. (1987) model, is an advantage (Liteplo et al., 1998); on the other hand, DPX assumes that formaldehyde is the reactive metabolite, a hypothesis for which there are fewer supporting data (Wheeler et al., 2001). Furthermore, the previous risk assessments have used limited data sets, and—in only one case—individual data from human subjects (Jonsson and Johanson, 2001). A recent publication by Sweeney et al. (2004) provided individual data for human subjects used by DiVincenzo and Kaplan (1981) to estimate group-mean kinetic parameters. These recent publications have led us to consider revising the cancer risk assessment by incorporating all available human exposure data sets in a Bayesian analysis. The previous paper by Marino et al. (2006) reported an improved mouse PBPK model for the traditional dosimeter for DCM of mg DCM metabolized by the GST pathway/L tissue/day using newer animal data and Bayesian statistics. We report here the results of calibration of that model with several studies of human volunteers (Åstrand et al., 1975; DiVincenzo and Kaplan, 1981; Engström and Bjurström, 1977; Stewart et al., 1972) and the estimation of unit risk factors using MCMC methodology.

2. Methods

2.1. Model structure

The PBPK model structure used for this analysis is the basic structure developed by Andersen et al. (1987, 1991) and refined by Marino et al. (2006) for the mouse, with a revision for humans to include extrahepatic/extrapulmonary metabolism (Fig. 1), as suggested by Sweeney et al. (2004). The model describes metabolism of DCM in both the liver and the lung by two competing pathways, an oxidative pathway and a glutathione conjugation pathway. The P450 (oxidative) pathway is described with saturable

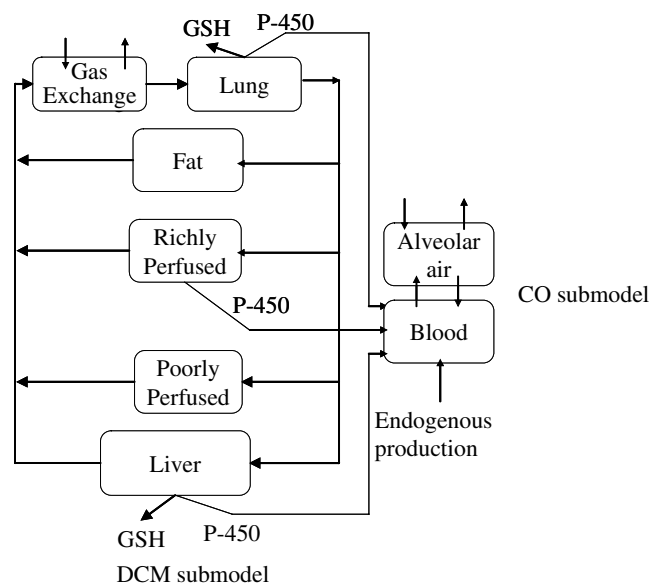


Fig. 1. PBPK model modified from Sweeney et al. (2004).

kinetics, while the glutathione *S*-transferase (GST) pathway is modeled as pseudo first-order. The model also includes a description of metabolism via an oxidative pathway in extrahepatic tissues other than the lung, represented in the model by the richly perfused tissue compartment.

For inhalation, it is assumed that the inhaled air in the lung and pulmonary blood quickly achieve steady-state, compared to the timeframe for distribution to tissues. The lung is described as two compartments: a gas exchange compartment and a metabolism compartment. This structure was assumed to allow for the equilibration of DCM between air and lung blood before it entered lung tissue (Andersen et al., 1987).

A lung dead-space parameter was added to the model to allow for human model prediction of exhaled air concentrations of DCM and CO (rather than including a fixed value for dead-space volume) for comparison with the available experimental data. Because of experimental difficulties associated with assuring that an air sample is entirely representative of “mixed exhaled air” collected over an entire exhalation or “end alveolar air” collected near the end of an exhalation, the dead-space parameter was allowed to vary during the analysis so that it could be estimated from each data set. In practice, it can be problematic to assure that the air collected from a particular subject is truly “mixed exhaled air” or “end alveolar air,” but modeling of exhaled air data depends critically on this distinction. End alveolar air is directly represented in the model, but to model-mixed exhaled air, it is necessary to calculate the weighted average of the air from the alveolar region and the air at the inhaled concentration from the dead space. For consistency, the model predictions for exhaled air are always calculated as the sum of the appropriate dead-space fraction times the inhaled concentration, plus one minus the dead-space fraction times the exhaled concentration. To predict mixed alveolar air, the full dead-space fraction (30%) is used, while to predict end alveolar air, the dead-space fraction is set to zero. The dead-space fraction was allowed to vary between 0 and 30%, with a mean of 15%, which is intermediate between the two standard collection approaches. In this way, the data itself was used to determine the contribution of dead-space air to the sample.

2.2. Data for Markov chain Monte Carlo (MCMC) analysis

Data from five human studies were used for calibration of the human model: a study by McKenna, summarized in Andersen et al. (1991); a study by DiVincenzo and Kaplan (1981); and studies by several government and academic investigators (Åstrand et al., 1975; Engström and Bjurström, 1977; Stewart et al., 1972). The data for the individual subjects in the study of DiVincenzo and Kaplan (1981) were described in Sweeney et al. (2004). Data for individual subjects from the studies used by Jonsson and Johanson (2001) (Åstrand et al., 1975; Engström and Bjurström, 1977). Each of these studies has different features that make it more or less appropriate for use in an MCMC analysis of the variability of DCM kinetics in humans. These features are summarized in Table 1. Because not

all parameters of exposure and analysis were comparable across the studies, the most useful data were incorporated into the model. The criteria for the usefulness of a particular data set for estimating metabolism parameters include: concentrations used with emphasis on concentrations relevant to the anticipated human environmental exposures, with exposures bracketing the saturation of metabolism, potentially more informative about metabolism parameters; duration of exposure with longer exposures being preferred; sampling times that encompass during- and post-exposure; and the biomonitoring analytes measured with emphasis on analytes that provide less variability, such as blood DCM compared to exhaled DCM. Based on these criteria, data from a total of 42 subjects were used for estimating metabolism parameters: 13 subjects from DiVincenzo and Kaplan (1981), which also include DCM and CO measurements in both blood and exhaled air that were obtained at the lowest exposure concentrations; 14 individuals from Åstrand et al. (1975); 12 subjects from Engström and Bjurström (1977) exposed to 750 ppm; and three individuals exposed to 514, 868, or 986 ppm from Stewart et al. (1972). Also included in the estimation of the metabolism parameters were group mean values at 100 and 350 ppm from Andersen et al. (1991). However, these data were not included in the analysis of variability.

As an initial evaluation of the comparability of these studies, a statistical analysis (ANOVA) was performed to evaluate variation in metabolism obtained at different exposures in the same study, as well as across studies (data not shown). To provide a basis for comparison, the peak concentration of each measured quantity (e.g., COHb, blood DCM, exhaled DCM, etc.) over the period of an experiment was divided by the nominal exposure concentration for that experiment. Only those studies that did not demonstrate a statistically significant difference were included in the MCMC analysis.

2.3. MCMC analysis

A hierarchical population model was developed, and Bayesian analysis was performed to quantify the uncertainty and variability in the PBPK model parameters for the human DCM model as recommended by Bernillon and Bois (2000). This approach separates individual and population levels of variability. Kinetic parameters were modeled at population and experiment levels of the hierarchical model with separate distributions for the population means and variances, while each physiological parameter, partition coefficient, and CO submodel parameter was modeled more simply with one distribution representing the experiment level mean and variability of the parameter. The experiment level distributions for physiological parameters, partition coefficients, and CO submodel parameters were not updated in the analysis because the population distributions for these parameters should not be redefined based on data from the relatively small number of subjects in the kinetic studies. Rather, these values are more properly estimated from the information in the general literature

Table 1
Summary of studies providing data on the kinetics of methylene chloride (DCM) in humans

	Andersen et al. (1991)	DiVincenzo and Kaplan (1981)	Åstrand et al. (1975)	Engström and Bjurström (1977)	Stewart et al. (1972)
Type of data	Summary	Individual	Individual	Individual	Summary/individual
Concentrations (ppm)	100 and 350	50 to 200	250 to 500	750	500 to 1000
Durations (h)	6	8	2.5	1	1 to 2
Time-points	During/post	During/post	During/post	Post	During/post
Measured:					
Exhaled DCM	Yes	Yes	Yes	Yes	Yes
Blood DCM	Yes	Yes	Yes	Yes	No
Fat DCM	No	No	No	Yes	No
Exhaled CO	Yes	Yes	No	No	No
Blood COHb	Yes	Yes	No	No	Yes

Listing of studies in which human subjects were exposed to methylene chloride (DCM) under controlled conditions. The form of the data presented is listed as summary mean or individual subject values; exposure concentrations and duration of exposure; and if the data were collected during or after (post) exposure. Also listed are the parameters that were measured such, as DCM or carbon monoxide (CO) in exhaled air; DCM or carboxyhemoglobin (COHb) in whole blood or plasma; or DCM in fat tissue.

that is based on a large number of subjects. The analysis was performed using MCSim (Bois et al., 2002), a publicly available implementation of MCMC analysis that is available at (http://toxi.ineris.fr/activites/toxicologie_quantitative/mcsim/mcsim.php#article3). The Metropolis–Hastings algorithm was used since it lends itself to PBPK models (Bernillon and Bois, 2000).

2.4. Prior distributions

Prior values were selected from multiple sources (Andersen et al., 1987, 1991; Bois, 2000; EPA, 2000; OSHA, 1997) reflecting, in each case, the source that was considered to represent the most current scientific evidence for each parameter. Mean values used to define the mean distributions for QCC, VPR, all tissue volumes except lung, and all tissue blood flows, were based upon values taken from the EPA Toxicological Review of vinyl chloride (EPA, 2000). The CVs of VPR and VLUC were set to values reported in OSHA (1997), while the CVs for all other human physiological parameters (Table 2) were set based on the values used for vinyl chloride (EPA, 2000). The means of the lung volume and all partition coefficients were taken from Andersen et al. (1987). Bounds for physiological parameters were 2½ standard deviations except where biologically implausible bounds resulted. The CO submodel parameter means (Table 3) were set equal to the values in Andersen et al. (1991) with two

exceptions: the endogenous rate of the production of CO (REnCO) and the background amount of CO (ABCOC). The initial PBPK model systematically overpredicted the data for DCM concentrations during exposure in DiVincenzo and Kaplan (1981) when the values from Andersen et al. (1991) for REnCO and ABCOC were used. This discrepancy, which is on the order of a factor of two, was particularly problematic because there was no apparent way to bring the model into agreement with the data except to use an implausibly low value of the blood:air partition coefficient. The model also tended to overpredict CO and COHb concentrations, but this discrepancy appeared to result partly from lower background levels of CO, and COHb in this study compared to the study summarized in Andersen et al. (1991). Adjustment of these background levels resulted in better agreement of the model predictions with the data for CO and COHb, particularly in view of the inability of the model to reproduce the DCM concentrations during the same period. To avoid possibly unrealistically high estimates of K_{FC} (given that the linear pathway does not produce CO, the increasing K_{FC} will decrease the predicted blood concentrations of DCM without increasing the predicted concentrations of CO and COHb), new estimates of REnCO and ABCOC, based upon the data from DiVincenzo and Kaplan (1981), were used to define the prior distributions. Andersen et al. (1991) provided the mean for V_{MaxC} and K_M (Table 4) but reported no mean values for A1 or A2; therefore, the means for A1 and A2 are from Andersen et al. (1987). The CVs for these

Table 2
Input parameters for the Monte Carlo analysis

Parameter		Distribution				
		Shape	Mean	Standard deviation	Lower bound	Upper bound
BW	Body weight (kg)	Normal	70.0 ^a	21.0	7.0	133.0
Flow rates						
QCC	Cardiac output (L/h/kg ^{0.74})	Normal	16.5 ^a	1.49	12.0	21.0
VPR	Ventilation/perfusion ratio	Lognormal	1.45 ^a	0.203 ^b	1.0	2.06
Fractional flow rates (fraction of cardiac output)						
QFC	Fat	Normal	0.05 ^a	0.0150	0.0050	0.0950
QLC	Liver	Normal	0.26 ^a	0.0910	0.010	0.533
QRC	Rapidly perfused tissues	Normal	0.50 ^a	0.10	0.20	0.80
QSC	Slow perfused tissues	Normal	0.19 ^a	0.0285	0.105	0.276
Fractional tissue volumes (fraction of body weight)						
VFC	Fat	Normal	0.19 ^a	0.0570	0.0190	0.361
VLC	Liver	Normal	0.026 ^a	0.00130	0.0221	0.0299
VLuC	Lung	Normal	0.0115 ^a	0.00161	0.00667	0.0163
VRC	Rapidly perfused tissues	Normal	0.064 ^a	0.00640	0.0448	0.0832
VSC	Slowly perfused tissues (muscle)	Normal	0.63 ^a	0.189	0.0630	1.20
Partition coefficients						
PB	Blood/air	Lognormal	9.7 ^c	0.970	7.16	13.0
PF	Fat/blood	Lognormal	12.4 ^c	3.72	4.92	28.7
PL	Liver/blood	Lognormal	1.46 ^c	0.292	0.790	2.59
PLu	Lung/arterial blood	Lognormal	1.46 ^c	0.292	0.790	2.59
PR	Rapidly perfused tissue/blood	Lognormal	1.46 ^c	0.292	0.790	2.59
PS	Slowly perfused tissue (muscle)/blood	Lognormal	0.82 ^c	0.164	0.444	1.46
Metabolism parameters						
V_{MaxC}	Maximum metabolism rate (mg/h/kg ^{0.7})	Lognormal	9.42	1.23	6.33	13.8
K_M	Affinity (mg/L)	Lognormal	0.433	0.146	0.154	1.10
A1	Ratio of lung V_{Max} to liver V_{Max}	Lognormal	0.000993	0.000396	0.000291	0.00292
A2	Ratio of lung K_F to liver K_F	Lognormal	0.0102	0.00739	0.00116	0.0580
FracR	Fractional MFO capacity in rapidly perfused	Lognormal	0.0193	0.0152	0.00190	0.122
1st Order metabolism rate (kg ^{0.3} /h)						
K_{FC}	Heterozygous	Normal	0.676	0.123	0.00	1.05
K_{FC2}	Homozygous	Normal	1.31	0.167	0.00	1.81

Physiological parameters used as inputs (priors) into the MCSim program.

^a Data taken from EPA (2000).

^b Data taken from OSHA (1997).

^c Data taken from Andersen et al. (1987).

Table 3
Prior distributions for human CO submodel parameters

Parameter		Mean	CV	Lower bound	Upper bound
Fractional tissue volume (fraction of body weight)					
VBI2C	Blood	0.059 ^a	0.30	0.0148	0.103
Miscellaneous parameters					
DLC	Diffusion coefficient for CO (L/h/mm Hg/kg ^{0.92})	0.058 ^a	0.39	0.01	0.1
ABCOC	Background amount of CO (mg/kg body weight)	0.1 ^b	7.5	0.01	1
REnCO	Rate of endogenous production of CO (mg/h/kg ^{0.7})	0.05 ^b	15	0.01	1
HBTot	Amount of hemoglobin (mmol/L)	10 ^a	0.05	9	11
M	Haldane coefficient (mm)	178.3 ^a	0.080	152	210
P1	CO yield factor	0.71 ^a	0.18	0.5	1
F1	CO elimination factor	0.85 ^a	0.15	0.5	1
COInh	Concentration of CO in air (ppm)	2.2 ^a	1.0	0	4.4

Physiological and metabolic parameters used as inputs (priors) into the MCSim program for the production of carbon monoxide (CO) from DCM.

^a Data taken from Andersen et al. (1991).

^b Estimated from data from DiVincenzo and Kaplan (1981).

Table 4
Individual calibrations of the human model kinetic parameter means^a

Parameter	Prior distributions		Posterior distributions											
			Andersen et al. (1991)		Åstrand et al. (1975)		DiVincenzo and Kaplan (1981)		Engström and Bjurström (1977)		Stewart et al. (1972)		Combined data sets	
	Mean	CV	Mean	CV	Mean	CV	Mean	CV	Mean	CV	Mean	CV	Mean	CV
V_{MaxC}	6.25	2	9.00	0.49	5.28	0.29	10.2	0.30	6.19	1.4	19.2	0.60	9.42	0.131
K_{M}	0.75	2	0.311	0.89	0.476	0.92	2.06	0.55	0.73	2.3	12.8	0.94	0.433	0.336
K_{FC}	2	2	2.84	2.1	7.95	1.5	5.87	0.59	34.0	2.0	1.92	1.9	0.852	0.711
A1	0.00143	2	0.00116	1.1	0.00104	0.58	0.00111	0.62	0.00103	0.61	0.00106	0.86	0.000993	0.399
A2	0.0473	2	0.0283	1.4	0.0127	1.0	0.0177	1.2	0.0155	1.1	0.0236	1.4	0.0102	0.728
FracR	0.03	2	0.0364	1.7	0.0184	1.3	0.0379	1.8	0.0224	1.3	0.0262	1.7	0.0193	0.786

^a Resulting mean metabolic values from the PBPK model when calibrated with data from each separate data set and when calibrated with individual values from all data sets combined. V_{MaxC} = Maximum metabolism rate (mg/h/kg^{0.7}); K_{M} = Affinity (mg/L); K_{FC} = first-order metabolism rate (kg^{0.3}/h); A1 = Ratio of lung V_{Max} to liver V_{Max} ; A2 = Ratio of lung KF to liver KF; FracR = Fractional MFO capacity in rapidly perfused tissues.

kinetic parameters are the default 200% as used by Bois (2000). The prior mean distribution for the extrahepatic/extrapulmonary metabolic parameter (FracR) was set to a small value of 0.03, which is slightly lower than was suggested by Sweeney et al. (2004). The upper bounds for all parameters were set at 2½ standard deviations with a few exceptions. The upper bounds for V_{MaxC} and K_{M} were 100 and 50, while the lower bounds were 0.1 and 0.05, respectively. These bounds were selected to maintain physiological plausibility but also were set large enough to avoid restricting the model too much. K_{FC} was bounded below by 0.01, and A1 and A2 were bounded by 0.0001. FracR was bounded above by 1.0 because extrahepatic metabolism is not expected to be greater than that in the liver and below by 0.0001.

2.5. MCMC simulation

Some minor modifications were made to the model to facilitate the varying inputs resulting from the distributional approach used in the MCMC simulations. The alveolar ventilation rate was correlated with the cardiac output by replacing the parameter QPC with a ventilation perfusion ratio (VPR) that is the ratio of the alveolar ventilation rate to the cardiac output. The fractional blood flows were constrained to sum to unity by dividing the fractional blood flow for each tissue by the sum of all the fractional blood flows. Likewise, the fractional tissue volumes were constrained to sum to 0.92, which is 100% minus a constant 8% carcass volume, by multiplying the fractional volume of each tissue by 0.92 and dividing by the sum of the sampled fractional tissue volumes.

Convergence of the Markov chains was monitored using analysis of variance as described by Gelman (1996). The estimated potential scale reduction, a ratio of an upper bound and a lower bound of the variance in

the target distribution, is used to diagnose convergence. In the limit, as the number of iterations of the Markov chains goes to infinity, the ratio declines to unity. In practice, simulation of two or three independent Markov chains is continued until the estimated potential scale reduction is less than 1.2 for the means of all parameters (Gelman, 1996).

2.6. Parameter identifiability

A qualitative identifiability analysis was conducted using a correlation matrix for all of the input parameters versus all of the corresponding estimates. Identifiability has to do with whether or not the parameters in the model can be estimated with some accuracy based on the data provided. An identifiable parameter is one that can affect the model output under the conditions of the simulation of the data being used for its estimation, and can therefore be estimated with some degree of certainty. To assess the identifiability of each parameter, correlation matrices were constructed based upon the last-lines output from each of the chains from the MCSim model runs. Only the experiment-specific parameter estimations were used because these best represent the data sets. Additional MCSim model runs were conducted that read in these parameter sets for each of the studies and output the value of the endpoints that were predicted for each parameter set at times to correspond to the actual measured data. For each of these studies, correlation coefficients were calculated for the interaction between each parameter and each estimated endpoint at each time; however, parameters for which experiment-specific measured values were used (i.e., ventilation rate) were not included. A qualitative identifiability analysis was conducted using a correlation matrix for all of the input parameters versus all of the corresponding estimates. The identifiability of the

parameters was assessed by examining the correlation coefficients between the parameters and the estimated endpoints from each of the individual kinetic studies for the human model. For this analysis, parameters with a correlation coefficient above 0.1 with the model predictions for several data points are considered to be potentially identifiable by these data (data not shown). Identifiable parameters were not overtly manipulated, but knowing which are identifiable provides some insight into parameters that influence the model outcome.

2.7. Cancer risk analysis

The PBPK model using the calibrated metabolic parameters was used to perform a cancer risk assessment for DCM, using the same tumor incidence and exposure concentration data relied upon in the current EPA (1991) IRIS entry. The current cancer risk analysis for DCM (EPA, 1991) provides a dose-response assessment for both inhalation and oral exposure with a PBPK model only considered in the derivation of the inhalation unit risk. For the derivation of the inhalation unit risk, EPA (1991) relied upon the combined incidence of adenomas and carcinomas in liver or lung reported in female mice in NTP (1986). Using this same bioassay data, the calibrated mouse and human models were applied to estimate unit risks for DCM. The human PBPK model was run based on continuous exposure to $1 \mu\text{g}/\text{m}^3$ for 7 weeks (1176 h). The average daily amount (mg) of DCM metabolized by the GST pathway/L tissue/day in the lung and liver for week 7 was then selected for subsequent unit risk calculations because steady state was achieved in week 7, i.e., the daily amount of DCM metabolized by the GST pathway/L tissue/day during week 7 was unchanged. This step yielded the average daily amount of DCM metabolized/ $(1 \mu\text{g}/\text{m}^3)$.

The application of the calibrated mouse PBPK model to estimate internal dose metrics was the same as that used by the EPA (1991) and OSHA (1997). The internal dose metric assumed to be associated with the effects observed in the animal bioassay, and thus with potential risks in the human, was mg DCM metabolized by the GST pathway/L tissue/day for both lung and liver tissue. The PBPK model predictions for the effective dose to the target tissues at the bioassay concentrations were used in place of administered dose as inputs for dose-response modeling. The human PBPK model results were then combined with “potency factors”, i.e., $0.1/\text{LED}_{10}$'s from the PBPK modeling of NTP (1986) and subsequent dose-response modeling to yield a distribution of unit risk factors. The PBPK modeling in the mouse was used to estimate the amount of DCM metabolized by the GST pathway at the treatment levels used in NTP (1986), i.e., 2000 and 4000 ppm. Dose-response modeling was then undertaken using these internal dose metrics from the PBPK modeling, i.e., mg DCM metabolized by the GST pathway/L tissue/day and the tumor incidence data from NTP (1986), in accordance with USEPA methodology. The resultant “potency factors” were used as described.

The intent of this effort was to develop an improved unit risk factor (URF) for DCM rather than conduct an environmental human health risk analysis of DCM. Once the URF is determined, this value could then subsequently be used for site risk assessment, air emission evaluations, etc., by selecting appropriate exposure factors (usually USEPA defaults) such as 350 d/year exposure frequency and 30 year exposure duration.

In the EPA analysis currently on IRIS, which was performed in 1987, scaling of the dose metrics by body surface area, which was the default approach at that time, was included in calculating the equivalent human doses. This factor is no longer considered appropriate when internal dose metrics based on PBPK modeling are used (EPA, 1992). Therefore, this factor was not included in the application of the calibrated models in this analysis.

2.8. Consideration of individual variability and GST-T1 polymorphisms

In addition to the application of the calibrated models to develop point estimates of unit risk, the final distributions of the model kinetic parameters in the human were applied in a Monte Carlo analysis to assess the

impact of variability in human pharmacokinetic parameters on predicted risks for a human population. The result is a distribution reflecting the potential variability of individual risks in the population.

The means and standard deviations used to define the parameter distributions for all kinetic parameters except K_{FC} for the Monte Carlo analysis were based upon the posterior distributions determined by the model calibration (Table 4). Since the distributions for the non-kinetic parameters were not updated in the calibration, the means and standard deviations used to define the distributions used in the Monte Carlo analysis were the same as those used to define the prior distributions in the MCMC analysis, with one exception: the mean value used for cardiac output was changed to be more representative of an average activity level among the general population. Given that study-specific body weights were available for most of the data used in the calibration, a distribution for body weight was not included in the MCMC analysis; however, a body weight distribution did need to be defined for the Monte Carlo analysis and was based upon a standard default distribution available for the general US population. Bounds were defined for all of the parameters as the mean ± 3 standard deviations, which would encompass approximately 99% of the distribution.

Distributions reflecting the genetic polymorphism in the GST pathway that metabolizes DCM (GST-T1) were also included in the Monte Carlo simulation. The polymorphism in GSTT1 has been well characterized, and Haber et al. (2002) (Table 5) reported population distribution of genotypes. Quantitative information on the relationship between the activities of the various genotypes of GST-T1 in a population of 208 healthy males and females from the southern and central parts of Sweden is presented in Warholm et al. (1994). The actual activities reported for methylene chloride were not used but rather, methyl chloride, a standard GST-T1 substrate, was used to determine the relationship between the relative activities for each of the various genotypes. The distributions of the activity for each genotype reported by Warholm et al. (1994) were scaled to obtain distributions of K_{FC} for each allele that, when weighted by the associated population frequencies (Haber et al., 2002) would result in an overall population mean equal to the posterior mean for K_{FC} obtained from the in vivo model calibration. This approach is the same as that applied in the Bayesian analysis for methylene chloride conducted by Jonsson and Johanson (2001). Unlike with the MCMC analysis, however, the distribution for K_{FC} was assigned to be normally distributed based upon the data from Warholm et al. (1994).

The approach used to evaluate potential variability in the risks associated with human inhalation exposure to DCM was to generate a distribution of the internal dose metric associated with the GST pathway (mg DCM metabolized by the GST pathway/L tissue/day) in the lung and the liver following continuous human exposure to $1 \mu\text{g}/\text{m}^3$ DCM in air. This Monte Carlo analysis was conducted using a Latin Hypercube sampling technique, with 3000 sets of values determined by sampling from each parameter distribution. The frequency of sampling from each GST activity distribution was determined by the prevalence of each genotype estimated in the US population. These distributions in internal dose metrics were converted to a distribution of unit risks by multiplying the dose metrics by internal dose metric risk factors developed using TOX_RISK (Version 5.3), i.e., the ratio of $0.1/\text{LED}_{10}$ for the corresponding endpoint, consistent

Table 5
Population distributions of GSTT genotypes^{a,b}

Population	Genotype frequency		
	+/+	+/-	-/-
Caucasian	0.31	0.49	0.19
African American	0.28	0.50	0.22
Hispanic	0.47	0.43	0.10
Asian American	0.05	0.33	0.62
US average	0.32	0.48	0.20

^a Table reproduced from Haber et al. (2002).

^b Adapted from data presented in El-Masri et al. (1999) assuming Hardy-Weinberg equilibrium, where “+” and “-” refer to the wild-type and null alleles, respectively.

with current EPA practice. The liver and lung endpoints were combined as in the EPA assessment.

3. Results

3.1. MCMC analysis

The human model was calibrated from the mouse model (Marino et al., 2006) using all the appropriate human data sets in a two-step approach:

1. Separate MCMC analyses would be performed using the data from each one of the studies.
2. MCMC would be performed using all of the data on individual subjects with the exception of the unpublished Åstrand data.

Each calibration consisted of four chains of 50,000 iterations, each with an output at every fifth iteration. The results of calibration with each separate data set, as well as data from all data sets combined, are presented in Table 4.

In the case of Åstrand et al. (1975) and Engström and Bjurström (1977) data sets, the model underpredicted the exhalation of DCM after the end of the last exposure period, which was due to the complex nature of the exposures (involving different activity levels) and the difficulties associated with trying to use measured ventilation rates

(Fig. 2). Specifically, the model changed from the ventilation rate measured during the last exposure period (which typically involves an increased level of activity) to the resting ventilation rate immediately at the end of the exposure. If allowance was made for a delay in the return of ventilation (and the associated blood flow) to the resting level, the model was able to reproduce the post-exposure period quite well. It was not clear how this artifact of the experimental protocol could be factored into the MCMC analysis. To avoid unrealistic posterior estimates of K_M using these data, the post-exposure data points were eliminated from the MCMC analyses for these individual data.

The results of the analysis of variance indicated that the data from different experiments in the same study appear to be consistent, with two exceptions: First, the two exposures in the Andersen et al. (1991) data were significantly different from each other; however, this is the only study in which exposure concentrations bracket the region of saturation of metabolism. Therefore, it is not surprising that the two exposures would provide different information. Second, Åstrand et al. (1975) experiment is different from the first, but not different from the second. This experiment was retained.

In addition, the comparison across studies tended to group the studies into three distinct clusters: one cluster of similar experiments included the three published Åstrand et al. (1975) experiments, all of the Engström and Bjurström (1977) experiments, and the higher exposure

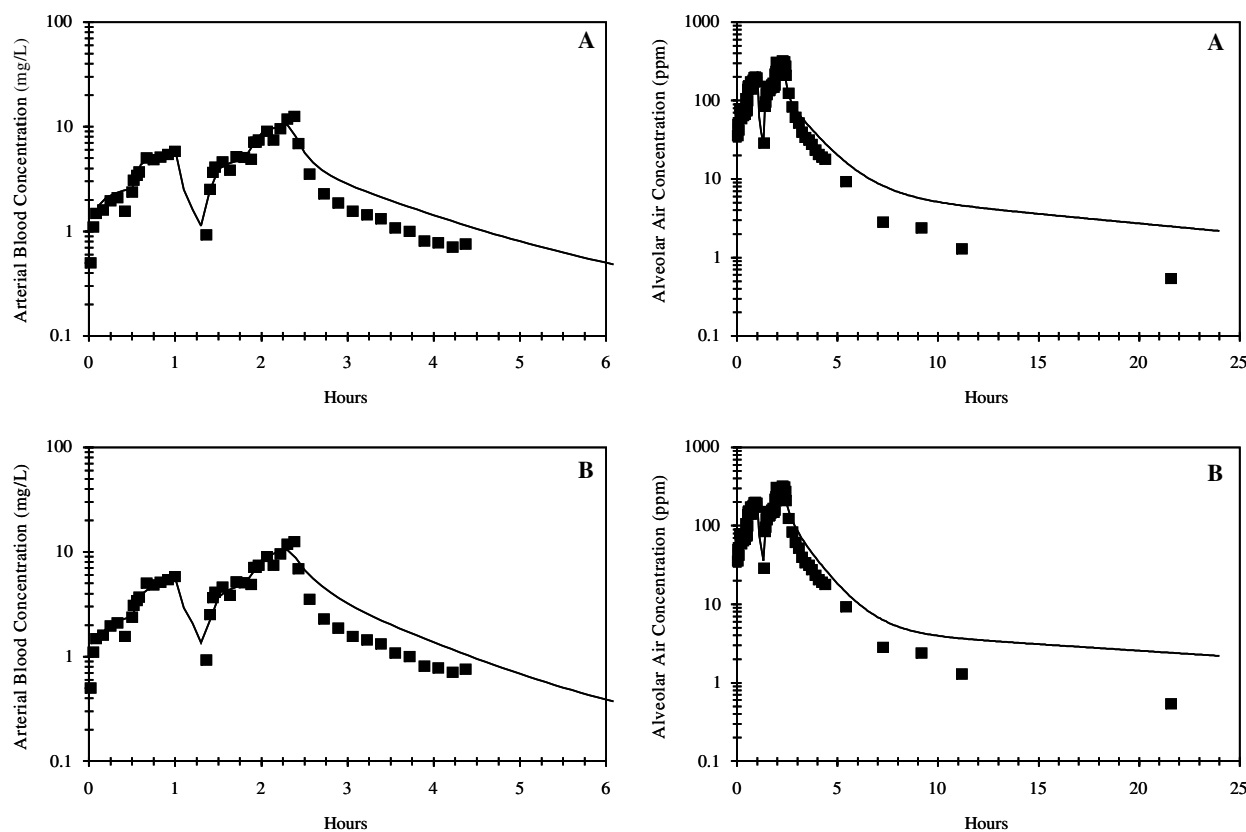


Fig. 2. Predicted (—) versus experimental (■) DCM blood and alveolar air concentrations in two human subject exposed to 500 ppm DCM. From Åstrand et al. (1975). Panel A shows predicted values from the model using prior estimates for metabolism. Panel B shows predicted values from the model using posterior estimates for metabolism.

concentration in Andersen et al. (1991). All of these experiments were conducted at concentrations above saturation of metabolism. The second cluster included the four experiments in DiVincenzo and Kaplan (1981), which are at concentrations below saturation, while the third included the highest concentration data—the three Stewart et al. (1972) experiments.

The results of the calibrations of the human model are shown in Table 4. Posterior distribution definitions were determined based upon a varying number of lines from the end of the output: 3000 lines for the data from Andersen et al. (1991); DiVincenzo and Kaplan (1981) and Stewart et al. (1972); 5000 lines for the Åstrand et al. (1975) data; 6000 lines for the Engström and Bjurström (1977) data; and 4000 lines for the combined individual data. The number of lines used for the averaging was the number of lines necessary so that the estimated potential scale reduction for all parameters was less than 1.2 for all parameters (Gelman, 1996). The use of longer chains was required in some cases to characterize the posterior distributions because of slow mixing in the chains. That is, the Markov chains moved very slowly across the target distribution, and it took more iterations of the chains to cover the spread of the distribution.

The variability in all population means was reduced with the calibration using the combined individual data. With the exception of A2, the prior mean is within three posterior standard deviations of the posterior mean for all parameters in Table 4; K_{FC} and A1 are within two standard deviations and FracR is within one standard deviation. The mean of A2 was decreased by a factor of almost five in the recalibration of the human model.

For the human simulations, extrahepatic/extrapulmonary metabolism was introduced in the richly perfused tissue via the FracR parameter. The prior for the mean of FracR specified a small amount of metabolic activity in this tissue compartment, 3% of the maximum rate of metabolism in the liver (V_{MaxC}). The posterior distribution from the combined calibration has an even smaller mean, approximately 2%, and the CV decreases by slightly more than half.

The CV at the mean of the distribution for the variance¹ for the combined calibration changes very little from the prior CV for all parameters, and the only increase is a slight one for FracR. The CVs for the variance distributions for the combined calibration decrease from approximately 30% for A2 to about 60% for V_{MaxC} .

3.2. Cancer risk analysis

When the human model was run using the mean values from the human posterior distributions, the point estimate of the unit risk (per $\mu\text{g}/\text{m}^3$) associated with liver adenomas or carcinomas was 6.06×10^{-10} , and the point estimate of unit risk associated with lung adenomas or carcinomas was 5.69×10^{-10} . The total unit risk is 1.18×10^{-9} , which is a factor of approximately 400 lower than the current EPA unit risk estimate of 4.7×10^{-7} . Of this 400-fold difference, approximately a factor of 13 is due to the inappropriate application of body surface area scaling in the EPA risk assessment. The other factor of approximately 30 reflects an increase in the estimated dose metric in the mouse of approximately 4-fold related to the re-estimation of the metabolic parameters, and a decrease in the estimated dose metric in the human of approximately 7-fold for the same reason.

¹ The CV at the mean of the distribution for the variance is the best estimate of the coefficient of variability for the parameters. It is calculated by dividing the square root of the best estimate of the variance (the mean of the distribution for the variance) by the best estimate of the mean (the mean of the distribution for the mean).

Table 6
Descriptive statistics of the dose metric distributions

	Total risk ^a	Liver risk	Lung risk
Mean	1.05×10^{-9}	5.31×10^{-10}	5.22×10^{-10}
SE	1.61×10^{-11}	7.75×10^{-12}	1.06×10^{-11}
Median	9.33×10^{-10}	4.78×10^{-10}	3.70×10^{-10}
SD	8.83×10^{-10}	4.24×10^{-10}	5.80×10^{-10}
Kurtosis	3.75	1.74	6.47
Skewness	1.33	0.98	2.17
Range	7.29×10^{-9}	3.00×10^{-9}	4.29×10^{-9}
Minimum	0	0	0
95th Percentile	2.70×10^{-9}	1.31×10^{-9}	1.66×10^{-9}
99th Percentile	3.75×10^{-9}	1.75×10^{-9}	2.75×10^{-9}
Maximum	7.29×10^{-9}	3.00×10^{-9}	4.29×10^{-9}
Count	3003	3003	3003

^a Cancer risk per $\mu\text{g}/\text{m}^3$ exposure concentration for the liver, lung, or for both organs (Total risk) using the calibrated PBPK model derived in this study.

nomas or carcinomas was 6.06×10^{-10} , and the point estimate of unit risk associated with lung adenomas or carcinomas was 5.69×10^{-10} . The total unit risk is 1.18×10^{-9} , which is a factor of approximately 400 lower than the current EPA unit risk estimate of 4.7×10^{-7} . Of this 400-fold difference, approximately a factor of 13 is due to the inappropriate application of body surface area scaling in the EPA risk assessment. The other factor of approximately 30 reflects an increase in the estimated dose metric in the mouse of approximately 4-fold related to the re-estimation of the metabolic parameters, and a decrease in the estimated dose metric in the human of approximately 7-fold for the same reason.

3.3. Consideration of individual variability and GST-T1 polymorphisms

The point estimate of unit risk described above does not consider the potential variability in risk in the general population. To consider the quantitative information available on the differences in GST activity in individuals with different genotypes, as well as on the variation in other pharmacokinetic parameters, a Monte Carlo analysis was conducted.

The descriptive statistics of the distribution of unit risks for the US population are provided in Table 6, with the SAS output provided in the supplemental information. It was found that 3000 iterations provided reproducible predictions (to two significant figures) of the 95th percentile of the distribution of dose metrics. The results indicate skewed distributions for liver and lung tumor risks, alone or in combination, with a mean unit risk of 1.05×10^{-9} , considering both liver and lung tumors. The unit risks range from 0 (which is expected because approximately 20% of the US population is estimated to be non-conjugators) up to a unit risk of 2.70×10^{-9} at the 95th percentile. The median or 50th percentile is 9.33×10^{-10} , which is approximately a factor of 500 lower than the current EPA unit risk of 4.7×10^{-7} . Because the distributions are skewed, the median, rather than the mean, would be more representa-

tive of an average individual in the population. It should be noted that this is a distribution of upper bound unit risk because it is based on the upper bound of the slope factor estimated from the benchmark dose modeling.

4. Discussion

This study provides a revised assessment of cancer risk for DCM using refined data for human metabolic and physiological parameters, state-of-the-science probabilistic methodology, and a GST-metabolite as the dose metric. The assessment provided here goes beyond previously published assessments in several ways. First, the metabolism of DCM from the CYP metabolic component has been improved using the analysis of Sweeney et al. (2004), which re-examined the metabolism of DCM in human volunteers (DiVincenzo and Kaplan, 1981). That re-examination provided better values for metabolic parameters because individual data were available compared with previous group means (Andersen et al., 1987), and a secondary extrahepatic/extrapulmonary component was added to account for higher DCM metabolism at low concentrations (<100 ppm). Furthermore, individual values for metabolism of DCM from all available human data sets were included to estimate the population parameters using probabilistic statistics; no previous PBPK models or risk assessments have attempted to combine all human data sets. Like El-Masri et al. (1999) and Jonsson and Johanson (2001), the calculation of risk incorporated the incidence of polymorphisms in glutathione transferase GST-T1 into the analysis, but the dose metric used by El-Masri et al. (1999) and Jonsson and Johanson (2001) focused on nucleic acid-protein cross-links (Casanova et al., 1997), while the current assessment follows the more traditional dose metric, i.e., the amount of DCM metabolized by the GST pathway/L tissue/day. Thus, the assessment presented here is a significant improvement in the determination of risk to the general population.

A comparison of unit risk values is provided in Table 7. The outcome of the analysis and the unit risk calculated differs from the original EPA value by a value of approximately 400. Of this difference, a factor of approximately 13 is due to the application of body surface area allometric scaling previously used by the EPA in their risk assessment of DCM. While this practice is no longer used by the EPA, some have argued that incorporating a surface area correction is consistent with PBPK modeling

(Rhomberg, 1995). Nonetheless, the fact that the EPA has modified its original proposal for the use of species scaling factors (EPA, 1992) and has elected to not incorporate such a factor in recent risk assessments suggests that this is a moot issue. Thus, the approach presented here is consistent with that used more recently by the USEPA for vinyl chloride, a cancer risk assessment using a PBPK model to predict dose metrics for a reactive metabolite (EPA, 2004), and with Bayesian statistical methodology (Bernillon and Bois, 2000). The other factor of approximately 30 reflects a summation of contributions such as an increase in the estimated dose metric in the mouse of approximately 4-fold, which is related to the re-estimation of the metabolic parameters, and a decrease in the estimated dose metric in the human of approximately 7-fold. Part of the differences stem from the use of the Bayesian probabilistic calculations, compared with the deterministic approaches previously used, and the incorporation of improved estimation techniques and metabolic parameters. Probabilistic methods are considered more amenable to heterogeneous populations than are deterministic methods because they account for the variability in the target population such that each parameter is assumed to have a random distribution for any given population rather than a true value that can easily be determined. Using probabilistic methods to estimate population values was proposed by Portier and Kaplan (1989), and was shown by them to improve the population estimates for DCM. Thus, the work presented here represents the state of the science for quantitative risk assessment of DCM.

The importance of using individual data from all human data sets, rather than selected data sets, which was proposed by Bois (1999), cannot be diminished especially in light of modern standards that preclude the collection of human data. Risk assessors are at an advantage with DCM to have such a large population covering a range of exposure concentrations. Furthermore, the advantage of values from individual subjects, rather than group means, allows for the full use of probabilistic statistics to estimate the true population means and variability. Such a large population of subjects serves to reduce the uncertainty associated with developing and using human data in risk assessments. That said, there is an assumption that these individuals represent the human population sufficiently to be used broadly. It is difficult to know with certainty that these individuals are representative of the human population, but Sweeney et al. (2004) showed that the metabolic parameters for the 13 subjects used by DiVincenzo and Kaplan demonstrated substantially different metabolism and was within population standard deviations reported by others. Regrettably, we cannot correlate that difference to induction of enzyme systems, or to genotype because these data are not available. This lack of information only emphasizes the uncertainty in relying on data generated decades ago: how accurate are the data, and how reliable are the measurements. Some of these uncertainties were

Table 7
Comparison of unit risk values

Risk	David et al.	EPA	El-Masri et al.	Jonsson and Johanson
Mean total risk	1.05×10^{-9}	4.7×10^{-7}	2.03×10^{-10}	2.03×10^{-10}
95th percentile	2.70×10^{-9}	Not available	4.94×10^{-10}	4.86×10^{-10}

Mean risk values for lung or liver cancer per $\mu\text{g}/\text{m}^3$ exposure to DCM calculated by the authors, US EPA (IRIS), El-Masri et al. (1999) or Jonsson and Johanson (2001).

taken into account in evaluating the data to be used in calibration of the model.

Another area of uncertainty concerns the model prediction of metabolism. Comparisons of the experimental data to model predicted values demonstrate that the model does well in predicting DCM metabolism at high concentrations. At lower concentrations, the model tended to underpredict metabolism which is why Sweeney et al. (2004) incorporated an additional CYP component into the poorly-perfused tissue compartment. In revising the Sweeney model, we elected to move the extrahepatic metabolism to the richly-perfused tissue compartment, and the MCSim analyses modified its contribution from 10% to ~3%. The assumption is that no other pathways are involved, and that induction of the CYP pathway is not a factor. These assumptions are not unique to the DCM PBPK model, however.

Risk estimates also reflect the impact of the GST polymorphism, although the impact is minor at the low end of the dose response. As stated above, previous assessments by El-Masri et al. (1999) and Jonsson and Johanson (2001) also incorporated GST polymorphisms. The impact of polymorphism can be dramatic for a GST-null population: as a result of the lack of activity in individuals with the null allele, the lower end of the population distribution is predicted to be at zero risk. The difference in activity between the homozygous and heterozygous wild alleles also serves to broaden the risk distribution: the 95th percentile of the population risk distribution is roughly 6-fold greater than the median risk. Previous analyses that did not consider the GST polymorphism predicted only a 3-fold difference between the 50th and 95th percentiles (Clewell et al., 1993; OSHA, 1997). But for the low of the dose response, these polymorphisms do not have much impact. A similar observation was made by Sakai et al. (2002), when looking at the correlation of urinary DCM with exposure in an occupational population.

A significant difference between the risk assessment presented here and previously published assessments is the use of GSH flux as the dose metric, rather than DPX formation, as was done by Casanova et al. (1996); El-Masri et al. (1999); Jonsson and Johanson (2001). The value of DPX might be uncertain given that it has only been demonstrated in mouse liver, but not in mouse lung (the other target organ) and not in human liver. The argument that DPX is at least measurable in one tissue, compared with the proposed reactive chloromethylglutathione metabolite proposed in the Andersen et al. (1987) model, is an advantage; on the other hand, DPX assumes that formaldehyde is the reactive metabolite, a hypothesis that does not have overwhelming data to support it (Wheeler et al., 2001). Recent studies by Marsch et al. (2001, 2004) suggest that the chloromethylglutathione is, indeed, possible to measure. Thus, while DPX is an attractive dose metric for risk assessment, it applies only to mouse liver, and not to mouse lung or human tissues. Furthermore, DPX assumes that carcinogenicity is the result

of formaldehyde formation, a hypothesis that might not have sufficient strength of evidence (Graves et al., 1994; Kayser and Vuilleumier, 2001).

Current EPA cancer risk assessment guidelines include a caveat to evaluate the risk of sensitive sub-populations, such as children. This component was not included into the analysis because the issue of children's sensitivity to cancer from exposure to DCM was recently reviewed (Clewell et al., 2004). Their analysis and review indicate that neonatal children up to age 5 years are less likely to be exposed to carcinogenic metabolites of DCM than are adults. This was based on the pharmacokinetics of blood DCM and metabolism to the reactive metabolite using the GST pathway. Furthermore, their analysis did not demonstrate significant differences in kinetics between men and women. Thus, the assessment presented here represents a conservative estimate of risk for all likely sensitive sub-populations.

Interpretation of exhaled air data for an inhaled volatile chemical, such as DCM, is complicated by the fact that absorption of the chemical takes place only in the alveolar region. This is why PBPK models for these chemicals use the alveolar ventilation rate rather than the total pulmonary ventilation rate (Ramsey and Andersen, 1984). The alveolar ventilation rate is generally taken to be roughly two-thirds of the total ventilation rate, based on the fact that the "dead-space" region of the lung—that is, the upper airways where no absorption occurs—accounts for roughly one-third of the lung airspace volume. The other one-third of the total ventilation is assumed to result in the cyclic inhalation and exhalation of the compound at the ambient concentration. Thus, exhaled air represents a combination of air from the dead space and the alveolar region. The first air exhaled is primarily from the dead space, where the concentration of the compound is still essentially at the inhaled concentration. The later fraction of exhaled air primarily represents air from the alveolar region, which has been equilibrating with the lung blood.

In summary, a revised quantitative risk assessment has been performed using state-of-the-science probabilistic methodology, improved metabolic parameters for CYP and GST activities, and improved physiological parameters. The outcome suggests that the unit risk is reduced by a factor of over 100. The validity of this lower risk estimate may await comparison to the combined epidemiological data for exposed populations, but the estimate is consistent with the mode of action and differences in metabolic activity of DCM in humans compared with rodents (Slikker et al., 2004b).

Acknowledgments

The authors express their appreciation to Mr. Eric Hack for his contribution to the analyses, and to Drs. Thomas Starr and M.W. Anders for their insightful suggestions and thoughts regarding the design and conduct of this effort and regarding the preparation of this manuscript.

References

- Andersen, M.E., Clewell III, H.J., Gargas, M.L., Smith, F.A., Reitz, R.H., 1987. Physiologically based pharmacokinetics and the risk assessment process for methylene chloride. *Toxicol. Appl. Pharmacol.* 14, 243–261.
- Andersen, M.E., Clewell III, H.J., Gargas, M.L., MacNaughton, M.J., Reitz, R.H., Nolan, R., McKenna, M., 1991. Physiologically based pharmacokinetic modeling with dichloromethane, its metabolite carbon monoxide, and blood carboxyhemoglobin in rats and humans. *Toxicol. Appl. Pharmacol.* 108, 14–27.
- Åstrand, I., Ovrum, P., Carlsson, A., 1975. Exposure to methylene chloride. I. Its concentration in alveolar air and blood during rest and exercise and its metabolism. *Scand. J. Work Environ. Health* 1, 78–94.
- Bernillon, P., Bois, F.Y., 2000. Statistical issues in toxicokinetic modeling: a Bayesian perspective. *Environ. Health Perspect.* 108, 883–893.
- Bois, F., 1999. Analysis of PBPK models for risk characterization. *Ann. NY Acad. Sci.* 895, 317–337.
- Bois, F., 2000. Statistical analysis of Clewell et al. PBPK model of trichloroethylene kinetics. *Environ. Health Perspect.* 108, 307–316.
- Bois, F., Maszle, D., Revzan, K., Tillier, S., Yuan, Z., 2002. MCSIM Version 5 beta 2. Available at <http://toxi.ineris.fr/activites/toxicologie_quantitative/mcsim/article3>.
- Casanova, M., Conolly, R.B., Heck, H.d'A., 1996. DNA-protein cross-links (DPX) and cell proliferation in B6C3F₁ mice but not Syrian golden hamsters exposed to dichloromethane: pharmacokinetics and risk assessment with DPX as dosimeter. *Fundam. Appl. Toxicol.* 31, 103–116.
- Casanova, M., Bell, D., Heck, H., 1997. Dichloromethane metabolism to formaldehyde and reaction of formaldehyde with nucleic acids in hepatocytes of rodents and humans with and without glutathione *S*-transferase T1 and M1 genes. *Fundam. Appl. Toxicol.* 37, 168–180.
- Clewell, H.J. III, Gearhart, J.M., Andersen, M.E., 1993. Analysis of the metabolism of methylene chloride in the B6C3F₁ mouse and its implications for human carcinogenic risk. Submission to OSHA Docket #H-071, Exhibit #96. January 15, 1993.
- Clewell III, H.J., Gentry, P.R., Covington, T.R., Sarangapani, R., Teeguarden, J.G., 2004. Evaluation of the potential impact of age- and gender-specific pharmacokinetic differences on tissue dosimetry. *Toxicol. Sci.* 79, 381–393.
- DiVincenzo, G.D., Kaplan, C.J., 1981. Uptake, metabolism, and elimination of methylene chloride vapor by humans. *Toxicol. Appl. Pharmacol.* 59, 130–140.
- El-Masri, H.A., Bell, D.A., Portier, C.J., 1999. Effects of glutathione transferase theta polymorphism on the risk estimates of dichloromethane to humans. *Toxicol. Appl. Pharmacol.* 158, 221–230.
- Engström, J., Bjurström, R., 1977. Exposure to methylene chloride. Content in subcutaneous adipose tissue. *Scand. J. Work Environ. Health* 3, 215–224.
- Environmental Protection Agency (EPA), 1985. Integrated risk information system: Dichloromethane. <www.epa.gov/iris/subst/0070.htm>.
- Environmental Protection Agency (EPA), 1986. Guidelines for carcinogen risk assessment. EPA/630/R-00/004.
- Environmental Protection Agency (EPA), 1991. Integrated risk information system: dichloromethane. <www.epa.gov/iris/subst/0070.htm>.
- Environmental Protection Agency (EPA), 1992. EPA request for comments on draft report on cross-species scaling factor for cancer risk assessment. *Fed. Regist.* 57, 24152.
- Environmental Protection Agency (EPA), 2000. Toxicological review of vinyl chloride. EPA.635R-00/004.
- Environmental Protection Agency (EPA). 2004. Integrated risk information system: vinyl chloride. <www.epa.gov/iris/subst/1001.htm>.
- Gelman, A., 1996. Inference and monitoring convergence. In: Gilks, W.R., Richardson, S., Spiegelhalter, D.J. (Eds.), *Markov chain Monte Carlo in practice*. Chapman & Hall/CRC, Boca Raton, Florida, pp. 131–143.
- Graves, R.J., Callander, R.D., Green, T., 1994. The role of formaldehyde and *S*-chloromethylglutathione in the bacterial mutagenicity of methylene chloride. *Mutat. Res.* 320, 235–243.
- Haber, L.T., Maier, A., Gentry, P.R., Clewell III, H.J., Dourson, M.L., 2002. Genetic polymorphisms in assessing interindividual variability in delivered dose. *Regul. Toxicol. Pharmacol.* 35, 177–197.
- Jonsson, F., Johanson, G., 2001. A Bayesian analysis of the influence of GSTT1 polymorphism on the cancer risk estimate for dichloromethane. *Toxicol. Appl. Pharmacol.* 174, 99–112.
- Kayser, M.F., Vuilleumier, S., 2001. Dehalogenation of dichloromethane by dichloromethane dehalogenase/glutathione *S*-transferase leads to formation of DNA adducts. *J. Bacteriol.* 183, 5209–5212.
- Liteplo, R.G., Long, G.W., Meek, M.E., 1998. Relevance of carcinogenicity bioassays in mice in assessing potential health risks associated with exposure to methylene chloride. *Hum. Exp. Toxicol.* 17, 84–87.
- Marino, D.J., Clewell, H.J. III, Gentry, P.R., Covington, T.R., David, R.M., Morgott, D.A., 2006. Bayesian PBPK and dose-response modeling of dichloromethane in mice. *Reg. Pharmacol. Toxicol.* (submitted).
- Marsch, G.A., Mundkowski, R.G., Morris, B.J., Manier, M.L., Hartman, M.K., Guengerich, F.P., 2001. Characterization of nucleoside and DNA adducts formed by *S*-(1-acetoxymethyl)glutathione and implications for dihalomethane–glutathione conjugates. *Chem. Res. Toxicol.* 14, 600–608.
- Marsch, G.A., Botta, S., Martin, M.V., McCormick, W.A., Guengerich, F.P., 2004. Formation and mass spectrometric analysis of DNA and nucleoside adducts by *S*-(1-acetoxymethyl)glutathione and by glutathione *S*-transferase-mediated activation of dihalomethanes. *Chem. Res. Toxicol.* 17, 45–54.
- National Toxicology Program (NTP), 1986. Toxicology and carcinogenesis studies of dichloromethane (methylene chloride) (CAS No. 75-09-2) in F344/N rats and B6C3F₁ mice (inhalation studies). NTP-TRS-306.
- Occupational Safety and Health Administration (OSHA), 1997. Occupational exposure to methylene chloride. *Fed. Regist.* 62, No. 7, pp. 1493–1619.
- Portier, C.J., Kaplan, N.L., 1989. Variability of safe dose estimates when using complicated models of the carcinogenic process. A case study: methylene chloride. *Fundam. Appl. Toxicol.* 13, 533–544.
- Ramsey, J.C., Andersen, M.E., 1984. A physiologically based description of the inhalation pharmacokinetics of styrene in rats and humans. *Toxicol. Appl. Pharmacol.* 73, 159–175.
- Rhomberg, L., 1995. Use of quantitative modelling in methylene chloride risk assessment. *Toxicology* 102, 95–114.
- Sakai, T., Morita, Y., Wakui, C., 2002. Biological monitoring of workers exposed to dichloromethane, using head-space gas chromatography. *J. Chromatogr. B* 778, 245–250.
- Slikker Jr., W., Andersen, M.E., Bogdanffy, M.S., Bus, J.S., Cohen, S.D., Conolly, R.B., David, R.M., Doerrer, N.G., Dorman, D.C., Gaylor, D.W., Hattis, D., Rogers, J.M., Setzer, R.W., Swenberg, J.A., Wallace, K., 2004a. Dose-dependent transitions in mechanisms of toxicity. *Toxicol. Appl. Pharmacol.* 201, 203–225.
- Slikker Jr., W., Andersen, M.E., Bogdanffy, M.S., Bus, J.S., Cohen, S.D., Conolly, R.B., David, R.M., Doerrer, N.G., Dorman, D.C., Gaylor, D.W., Hattis, D., Rogers, J.M., Setzer, R.W., Swenberg, J.A., Wallace, K., 2004b. Dose-dependent transitions in mechanisms of toxicity: case studies. *Toxicol. Appl. Pharmacol.* 201, 226–294.
- Stewart, R.D., Fisher, T.N., Hosko, M.J., Peterson, J.E., Baretta, E.D., Dodd, H.C., 1972. Experimental human exposure to methylene chloride. *Arch. Environ. Health* 25, 342–348.
- Sweeney, L.M., Kirman, C.R., Morgott, D.A., Gargas, M.L., 2004. Development of a refined physiologically based pharmacokinetic model for dichloromethane and application to estimation of interindividual variation in oxidative metabolism in human volunteers. *Toxicol. Lett.* 154, 201–216.
- Warholm, M., Alexandrie, A., Hogberg, J., Sigwardsson, K., Rannug, A., 1994. Polymorphic distribution of glutathione transferase activity with methyl chloride in human blood. *Pharmacogenetics* 4, 307–311.
- Wheeler, J.B., Stourman, N.V., Armstrong, R.N., Guengerich, F.P., 2001. Conjugation of haloalkanes by bacterial and mammalian glutathione transferases: mono- and vicinal dihaloethanes. *Chem. Res. Toxicol.* 14, 1107–1111.